Mahalingam, R., and M. A. Valle, "Momentum Transfer in Two-Phase Flow of Gas-Pseudoplastic Liquid Mixtures," *Ind. Eng. Chem. Fundamentals*, 11, 470 (1972).
Middleman, S., *The Flow of High Polymers*, Interscience, New York (1968).
Oliver, D. R., and A. Young Hoon, "Two-Phase Non-Newtonian Flow," *Trans. Inst. Chem. Engrs.*, 46, T106 (1968).
Taitel, Y., and A. E. Dukler, "A Model For Predicting Flow Regime Transitions in Horizontal and Near Horizontal Gas-Liquid Flow," *AIChE J.*, 22, 47 (1976).
Tyagi, K. P., and R. P. S. Srivastava, "Flow Behavior of non-Newtonian Liquid-Air in Annular Flow," *Chem. Eng. J.*, 11, 147 (1976).
Weinberger, C. B., and J. D. Goddard, "Extensional Flow Behavior of Polymer Solutions and Particle Suspensions in a Spinning Motion," *Intern. J. Mult. Flow*, 1, 465 (1974).

Manuscript received March 31, 1978; revision received September 22, and accepted October 5, 1978.

Enhancement of Heat Transfer and Thermal Homogenity With Motionless Mixers

E. B. NAUMAN
Xerox Corporation
Xerox Square
Rochester, New York 14644

Motionless mixers are well suited to augment heat transfer and to provide a uniform thermal environment in laminar flow reactors. Heat transfer performance can be characterized with the Nusselt number, while the degree of thermal homogeneity can be characterized using the thermal time distribution which is the nonisothermal analogue of the residence time distribution. Theoretical results, calculations, and design strategies are presented for a variety of mixer types including flow inverters as well as the more common flow dividers. Two-channel, partial flow inversion is an excellent, near optimal, strategy for cooling or other situations such as polymerizations which give elongated velocity profiles. For flattened velocity profiles, perfect mixing can sometimes give better results. In practice, however, partial inverters can be expected to outperform those motionless mixers which are primarily flow dividers.

SCOPE

Laminar flow heat exchange is characterized by large temperature gradients within the fluid and by rather low heat transfer coefficients. In reacting systems, this nonuniform environment can give rise to large concentration gradients. A standard means of increasing heat transfer and of providing more uniform reaction conditions is to use multitube or extended surface heat exchangers, but these are expensive and may give rise to flow instabilities, particularly for polymerizations. An alternate, more recently emerging technology is to use motionless mixers installed within the flow duct. These are static devices which use the energy of the flowing fluid to promote mixing throughout the cross section of the duct. A typical device divides and recombines the flow stream, reducing the striation thickness by a factor of two or more for each elemental unit of the mixer. A series combination of such elements can approach homogeneity on a molecular scale, but even these nearly perfect mixers do not provide the best means for enhancing heat transfer. Instead, relatively simple devices known as a flow inverters maximize the driving force for heat transfer by interchanging material between the centerline and the walls.

When the length of the motionless mixer is short compared to the total length of the heat exchanger, heat transfer performance can be characterized in some detail. If the velocity profile is independent of axial position, that is, if fluid properties are nearly constant, rather powerful analytical techniques give optimal design parameters and optimal mixer locations for arbitrary flow geometries and fluid rheologies. If fluid properties are temperature sensitive or if highly accurate estimates of the Nusselt number are desired, numerical calculations are necessary, but a considerable degree of generalization and a reasonably robust design strategy remain possible. This strategy offers significant improvements in performance without lengthy optimization studies.

CONCLUSIONS AND SIGNIFICANCE

Commercial motionless mixers are difficult to analyze theoretically owing to complicated three-dimensional flows and the accompanying lack of symmetry. This paper takes a first step toward rigorous analysis by dividing the overall mixing process into simpler components of flow inversion and symmetry preserving flow division. The analysis shows an inherent weakness of flow division for augmentation of heat transfer coefficients. Better, nearly optimal results can be achieved with a practical, low pressure drop device known as the two-channel partial flow inverter. For parabolic and elongated velocity profiles, this device has the same asymptotic performance as a perfect mixer and outperforms a perfect mixer for all intermediate values of the Graetz parameter. For Graetz parameters above about 10 (Graetz numbers above 30), a single flow inverter installed midway in a heat exchanger will give a 25 to 30% improvement in Nusselt number. Larger enhancements in Nu are possible in a multizone heat exchanger with two or more flow inverters, but for very long heat exchangers, the best practical strategy is to intersperse an occasional motionless mixer of the conventional flow division type.

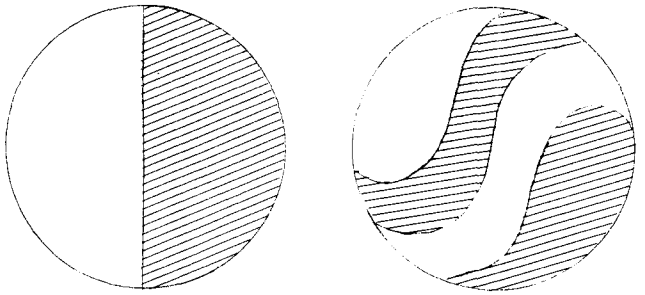

Fig. 1. Inlet to outlet transformation for typical motionless mixers.

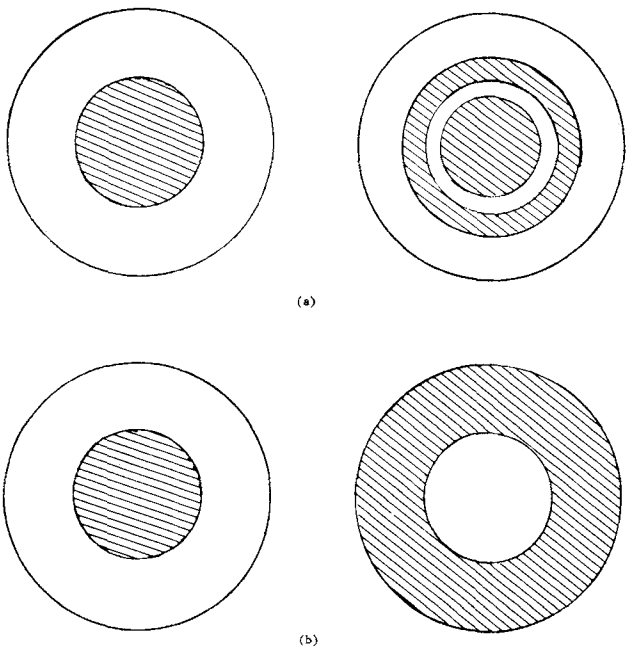

Fig. 2. Symmetry preserving transformations: (a) flow division (b) flow inversion.

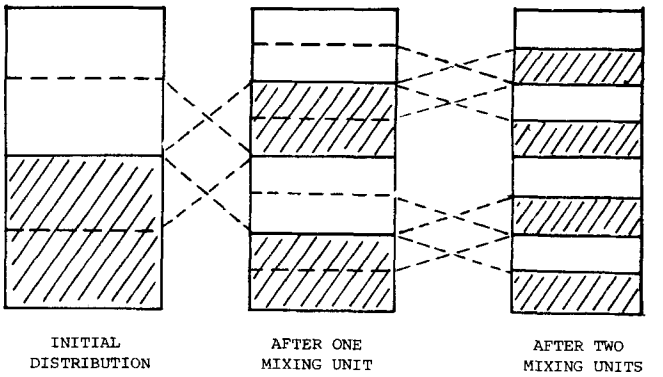

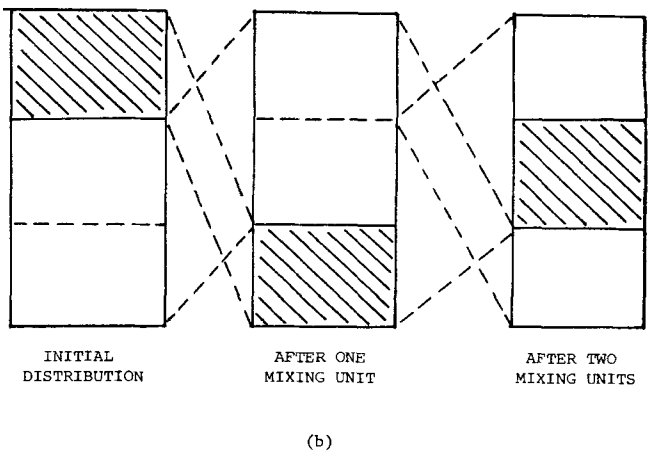

Fig. 3. Q-Space representation of symmetry preserving motionless mixers: (a) flow division (b) partial flow inversion.

Motionless mixers can be defined as a collection of static mixing elements installed within a flow duct. By changing flow fields and velocity profiles they redistribute fluid across the flow channel and thus rearrange temperature and composition distributions. There are a number of commercial, proprietary devices which are sold to enhance heat transfer and to provide a more uniform thermal and compositional environment for fluids in laminar flow. In many applications, the static mixing elements are distributed throughout the axial length of the heat exchanger or reactor. Thus, fluid is constantly rearranged through radial and tangential velocity components while predominately flowing in the axial direction down the duct. An application where the fluid is in more or less continuous contact with the static mixing elements is defined as a distributed motionless mixer. Such devices are usually effective in eliminating severe temperature and composition gradients but have high capital costs and high pumping costs compared to the open duct.

An economically attractive alternate to using distributed motionless mixers for reactors or heat exchangers is to use a lumped design where one or more localized mixers are separated by relatively long lengths of open pipe. One purpose of this paper is to analyze such systems and to present correlations of general utility. A second purpose is to introduce a new type of motionless mixer which provides superior heat transfer performance relative to commercial devices. A final purpose is to characterize lumped motionless mixers in a manner which allows simplified mathematical treatment and which is hopefully a first step toward rigorous analysis of motionless mixers in general.

MOTIONLESS MIXERS

Conventional motionless mixers give rise to complicated three-dimensional flows. Although it can be anticipated that numerical solutions for the laminar, isothermal flow of a Newtonian fluid will soon be available, these solutions will be of little direct utility in analyzing problems involving heat transfer or reaction if such effects are important within the mixer itself. However, if the mixer is short compared to the length of the total system, it may be possible to ignore heat and mass transfer effects within the mixer. Thus, the action of the mixer can be modeled as a transformation or mapping from an inlet plane to an outlet plane. Fluid which enters the mixer at some position (r_1, θ_1) will leave at position (r_2, θ_2). Figure 1 illustrates such a transformation.

Corresponding to this rearrangement of fluid will be a change in the spacial distribution of fluid properties which, in turn, leads to a change in velocities $\vec{V}_1(r_1, \theta_1, Z_1) \neq \vec{V}_2(r_2, \theta_2, Z_2)$. Entrance lengths in laminar flow tend to be quite short. Thus, if the mixer does not introduce too great an asymmetry, the velocity distribution at the mixer outlet will rapidly approach the fully developed profile $V_2(r)$ which corresponds to the rearranged physical properties. In this situation, heat, mass, and momentum trans-

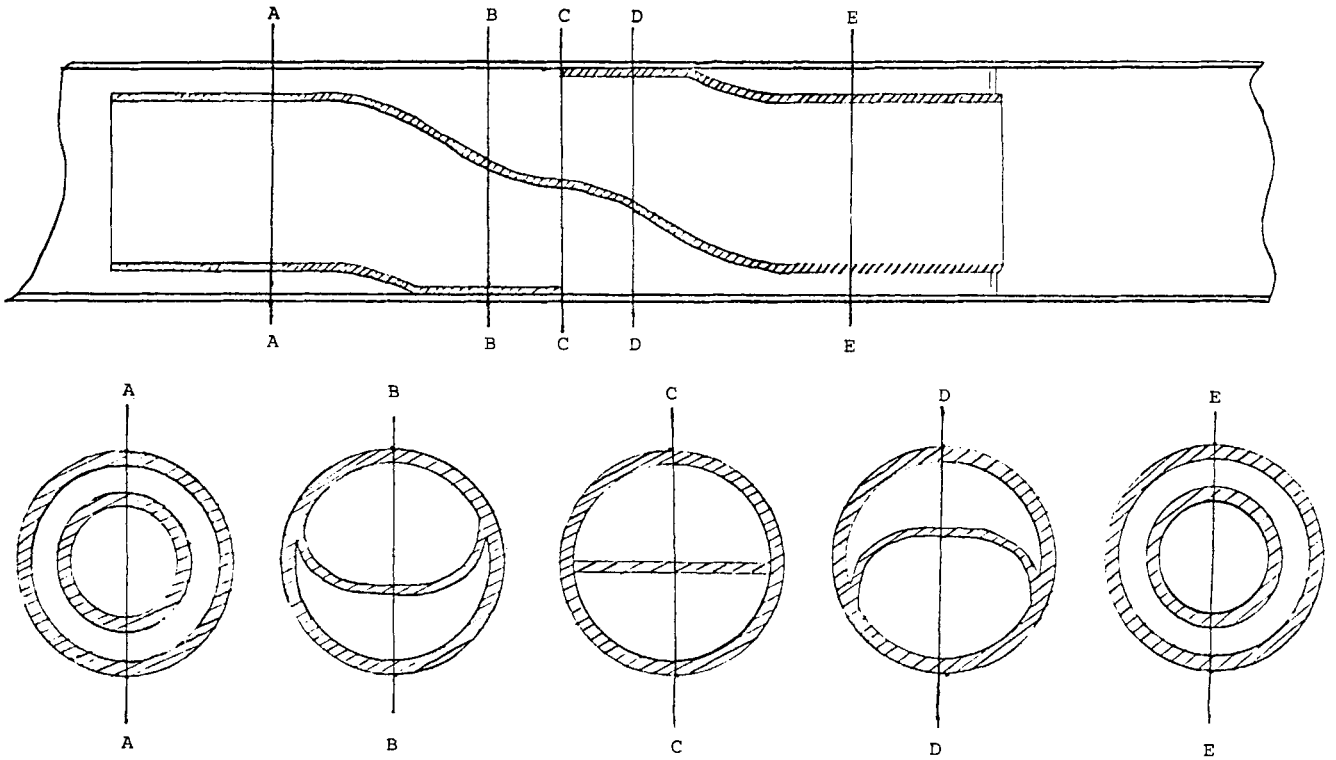

Fig. 4. Two-channel partial flow inverter.

fer downstream from the mixer will be governed by relatively simple boundary value problems.

It is clear that the analyses of motionless mixers would be much easier if they preserved radial symmetry. Existing commercial mixers destroy symmetry, but many aspects of their performance can be characterized by hypothetical flow devices which do preserve it. Figure 2*a* illustrates the inlet to outlet transformation for a flow divider which preserves radial and tangential symmetry, while Figure 2*b* illustrates a flow inverter. Actual physical devices can be constructed which yield transformations closely approximating those shown in Figures 2*a* and *b*. One of these, the flow inverter, turns out to be a practical, low pressure drop device, which outperforms existing motionless mixers for heat transfer applications.

Flow Division

The transformation illustrated in Figure 2*a* represents a single unit of the symmetry preserving flow divider. Subsequent units continue the division process, so that after N_e units the striation thickness is approximately

$$S = 2^{-(N_e+1)}\, R \tag{1}$$

The reason why Equation (1) is only an approximation is that each static element divides the stream according to volumetric flow rate, not radial position.

It is convenient to define a volumetric flow variable by

$$q(y) = \int_0^y W(y')\, V(y')\, dy' \tag{2}$$

Thus, the transformation in Figure 2*a* can be represented independently of the specific forms for W and V:

$$\begin{aligned} q(y_2) &= q(y_1) \quad , && 0 < q(y_2) < \tfrac{1}{4} \\ q(y_2) &= q(y_1) - \tfrac{1}{4}, && \tfrac{1}{4} < q(y_2) < \tfrac{1}{2} \\ q(y_2) &= q(y_1) + \tfrac{1}{4}, && \tfrac{1}{2} < q(y_2) < \tfrac{3}{4} \\ q(y_2) &= q(y_1) \quad , && \tfrac{3}{4} < q(y_2) < 1 \end{aligned} \tag{3}$$

Figure 3*a* gives a q space representation of this transformation. For parabolic flow in a round tube, the radial positions corresponding to $q = \frac{1}{4}, \frac{1}{2}, \frac{3}{4}$ are $y = 0.366$, 0.541, 0.707.

An important fact to note about symmetric flow division is that, regardless of the number of units in series, the material initially nearest the center remains at the center and the material initially nearest the wall remains at the wall. The ultimate consequence of this is that flow dividers are a comparatively poor method for improving heat transfer.

Flow Inversion

Figure 3*b* shows a typical example of flow inversion. The general transformation for this type of flow inversion is

$$\begin{aligned} q(y_2) &= q(y_1) - q(y_c) \quad , && q_2 < q_c \\ q(y_2) &= q(y_1) + 1 - q(y_c), && q_2 > q_c \end{aligned} \tag{4}$$

where $q_c = q(y_c)$ is a parameter governed by the specific design of the inverter. The coordinate y_d represents the radial position at which the entering fluid is divided between two flow channels, while the coordinate y_c represents the radial position at which the streams are combined after inversion, y_d and y_c being related by

$$q(y_d) = 1 - q(y_c) \tag{5}$$

Figure 3*b* shows the results after one and two stages of inversion for the specific case $q_d = 1/3$, $q_c = 2/3$. The corresponding radial positions for parabolic flow in a round tube are $y_d = 0.428$, $y_c = 0.650$. In this particular situation, a third stage of inversion would restore the fluid to its initial, undisturbed position. Unlike flow dividers, flow inverters should not be used in closely coupled, series combinations. Instead, they are used as the individual, isolated units in lumped motionless mixers. Also, unlike flow dividers, inverters do interchange material between the tube walls and the tube center.

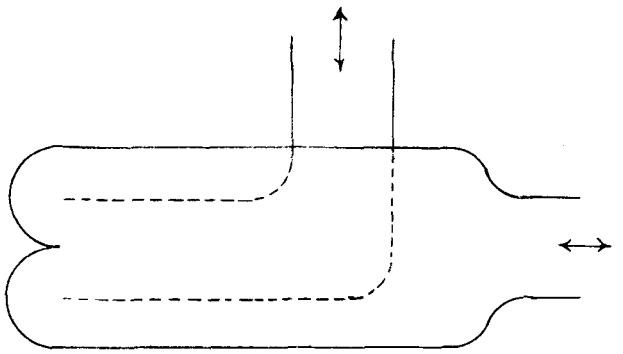

Fig. 5. Schematic design for complete flow inverter.

Physical devices which give close approximations to the transformation in Equation (4) are relatively easy to construct. A typical design is shown in Figure 4. This design is for $q_d = q_c = \frac{1}{2}$ so that the inverter is axisymmetric with $y_d = y_c = 0.541$. Design considerations for asymmetric flow inverters are discussed in Appendix A.

Flow inverters of the type shown in Figure 4 and repsented by the transformation in Equation (4) are two-channel partial inverters with only two regions of the fluid stream being interchanged in position. However, the general concent can be extended to three, four, or more channels. In the limit of many channels, the fluid is literally turned inside out so that the inversion

$$q(y_1) = 1 - q(y_2) \tag{6}$$

holds for every set of points y_1 and y_2. A physical device which closely approximates Equation (6) could, in fact, be constructed, and Figure 5 gives a schematic design for such a device. It is not suggested that complete flow inversion is a practical approach for actual heat exchangers or reactors. Like the symmetry preserving flow division discussed earlier, complete inversion is primarily useful as a mathematical abstraction. Together, complete inversion, partial inversion, and flow division possess the basic mixing characteristics of real motionless mixers without having the almost intractable asymmetries caused by strong radial and tangential flows. However, the two-channel partial inverter shown in Figure 4 is also a practical device, and it turns out to give heat transfer enhancements almost comparable to complete inversion and substantially better than flow division.

ANALYTICAL RESULTS

Graetz Problem With Intermediate Mixing

The classical Graetz problem governs heat transfer to a fluid with a parabolic velocity distribution flowing in a circular tube with walls held at constant temperature. The present analysis considers a similar but two-zone heat exchanger where, between zones, the fluid undergoes an instantaneous change in position. In much of the analysis it will not be necessary to confine the mathematics to parabolic velocity distributions or to circular coordinates, although for analytical results we will require that $V_x(r)$ be independent of x, assuming, in effect, constant physical properties. We begin by writing the governing equation in the general form:

$$v_x(r)\,\frac{\partial t}{\partial x} = \alpha\left(\frac{\partial^2 t}{\partial r^2} + \frac{g}{r}\,\frac{\partial t}{\partial r}\right) \tag{7}$$

where $g = 0$ for flat ducts and $g = 1$ for round tubes. The boundary conditions are $t = t_o$ for $x = 0$, $t = t_w$ at $r = R$, and $dt/dr = 0$ at $r = 0$. Equation (7) is more easily treated in dimensionless form. Let

$$T = \frac{t - t_w}{t_o - t_w}, \quad y = \frac{r}{R}, \quad z = \frac{x}{L}, \quad V = \frac{v_x}{\overline{V}} \tag{8}$$

then

$$\left(\frac{\overline{V}\,R^2}{\alpha\,L}\right) V(y)\,\frac{\partial T}{\partial z} = \frac{\partial^2 T}{\partial y^2} + \frac{g}{r}\,\frac{\partial T}{\partial y} \tag{9}$$

with boundary conditions

$$\begin{aligned} T &= 1 \quad \text{at} \quad z = 0 \\ T &= 0 \quad \text{at} \quad y = 1 \\ \frac{dT}{dy} &= 0 \quad \text{at} \quad y = 0 \end{aligned} \tag{10}$$

The dimensionless group in Equation (9) is defined as the Graetz parameter Pg. This group arises naturally in the problem and is widely used in the more mathematically oriented literature. It applies equally well to flat or round geometries and seems preferable to the Graetz number commonly employed for empirical correlations. The two dimensionless groups are related by

$$Pg = \frac{\overline{V}\,R^2}{\alpha\,L} = \frac{G_z}{\pi} \tag{11}$$

Note that Pg is defined in terms of the tube radius or the half width of a duct. Thus, it is four times smaller than the Φ group used by Jakob (1949).

Equation (9) is amenable to the classical technique of separating variables. Suppose

$$T(z, y) = Z(z)\,Y(y) \tag{12}$$

Then, it must be that

$$\frac{Pg}{Z}\,\frac{dZ}{dz} = -\lambda_n^2 = \frac{1}{VY}\left[\frac{d^2Y}{dy^2} + \frac{g}{y}\,\frac{dY}{dy}\right] \tag{13}$$

where λ_n are separation constants independent of z and y. Note that some authors use the center velocity V_o in defining the group Pg, so that their separation constants differ from the above by a factor of $V_o/\overline{V}$.

The solution for Z is the simple exponential

$$Z = \text{Exp}\,(-\lambda_n^2\, z/Pg) \tag{14}$$

while the solution for Y is a set of orthogonal eigenfunctions $Y(y)$ which satisfy the Sturm-Liouville problem represented by the right-hand side of Equation (13) together with its boundary conditions. The specific nature of the eigenfunctions depends on g and on the functional form for $V(y)$. A number of literature examples are discussed in Appendix B. For present purposes, a specific form for Y_n is not required.

The solution to Equation (9) is

$$T(z, y) = \sum_{n=0}^{\infty} C_n\,Y_n(y)\,\text{Exp}(-\lambda_n^2 z/Pg) \tag{15}$$

where the constants C_n must be picked to satisfy the boundary conditions at $z = 0$:

$$T(0, y) = \sum_{n=0}^{\infty} C_n\,Y_n(y) \tag{16}$$

The individual C_n can be found from noting that the Y_n are orthogonal with respect to the weighting function $W(y)V(y)$. That is

$$\int_0^1 W(y)\,V(y)\,Y_n\,Y_m\,dy = 0, \quad m \neq n$$

$$= N(\lambda_n), \quad m = n \tag{17}$$

where $N(\lambda_n)$ is a normalization parameter. Thus, multiplying Equation (16) by WVY_n and integrating from 0 to 1 gives

$$C_n = \frac{1}{N(\lambda_n)} \int_0^1 T(0, y)\, W\, V\, Y_n\, dy = \frac{F(\lambda_n)}{N(\lambda_n)} \tag{18}$$

where $T(0, y) = 1$ for the boundary condition of Equation (10).

Equations (15) and (18) together give the solution of the generalized Graetz problem for the first zone of the two-zone heat exchanger, that is, for $0 < z < z_I$. A motionless mixer is installed at axial position z_I, and this mixer rearranges the temperature from $T_1(z_I, y_1)$ before the mixer to $T_2(z_I, y_2)$ after the mixer.

Thus, the Graetz problem must be resolved with the new boundary condition $T_2 = T_1(z_I, y_2)$ at $z = z_I$. Proceeding in a manner similar to the above, we get

$$T_2(z, y_2) = \sum_{m=0}^{\infty} C_m\, Y_m(y_2)\, \mathrm{Exp}\,[-\lambda_m^2\,(z - z_I)/Pg] \tag{19}$$

where

$$C_m = \frac{1}{N(\lambda_m)} \int_0^1 T_1\,(z_I, y_1)\, WVY_m dy_2 \tag{20}$$

$$= \sum_{n=0}^{\infty} \frac{F(\lambda_n)\, I(\lambda_m, \lambda_n)}{N(\lambda_m)\, N(\lambda_n)} \mathrm{Exp}\,[-\lambda_n^2\, z_I/Pg]$$

where $F(\lambda_n)$ is defined by Equation (18), and

$$I(\lambda_m, \lambda_n) = \int_0^1 W(y_2)\, V(y_2)\, Y_m(y_2)\, Y_n(y_1)\, dy_2 \tag{21}$$

In a formal sense, Equations (19), (20), and (21) together constitute the solution of the generalized Graetz problem with a lumped motionless mixer at the intermediate point z_I, $0 < z_I < 1$. All that remains is to integrate Equation (21) using eigenfunctions appropriate to the geometry and velocity profile and using a transformation $y_1 \rightarrow y_2$ which represents the mixer. In practice, this integration is exceedingly difficult in a manipulative sense, even though the various eigenvalues and eigenfunctions are known. Appendix C gives a solution for the special case of flat duct with flat velocity profile, where the eigenfunctions are particularly simple: $Y_n = \cos\lambda_n y$, $\lambda_n = (2n + 1)\,\pi/2$. However, we do not require specific results for the formal analysis that follows and will use finite-difference calculations for the numerical results given later in this paper.

Optimal Mixing Parameters

Given a heat exchanger of fixed length $z = 1$, at what intermediate point $0 < z_I < 1$ should the motionless mixer be installed? If several mixers are to be used, what is their best spacing? These questions can be answered in rather surprising generality. We consider three cases:

1. The mixer is a two-channel partial flow inverter. In this case, the optimal value for q_c is also needed.
2. The mixer is a complete flow inverter.
3. The flow stream is perfectly mixed at the point z_I, this corresponding to the limit of a large number of flow dividers in series.

For a circular tube, the arithmetic mean Nusselt number can be expressed in terms of Pg and the dimensionless temperature $\overline{T}$ by

$$Nu = \frac{h_{ia} D}{k} = pPg \left[\frac{1 - \overline{T}}{1 + \overline{T}}\right] \tag{22}$$

where

$$\overline{T} = \int_0^1 W\, V\, T_2(1, y)\, dy$$

$$= \sum_{m=0}^{\infty} \sum_{n=0}^{\infty} \mathrm{Exp}\left[\frac{-\lambda_m^2\,(1 - z_I) - \lambda_n^2\, z_I}{Pg}\right] \frac{F(\lambda_m)\, F(\lambda_n)\, I(\lambda_m, \lambda_n)}{N(\lambda_m)\, N(\lambda_n)} \tag{23}$$

and where

$$F(\lambda_m) = \int_0^1 WVY_m\, dy \tag{24}$$

Note that the formulation of Equation (22) depends on the geometry, but that this has been included through the factor $p = 2$ for round tubes and $p = 4$ for flat plates.

Maximization of Nu is equivalent to minimizing $\overline{T}$ for a fixed L. We shall show that

$$\frac{\partial \overline{T}_2}{\partial z_I} = \frac{\partial \overline{T}}{\partial q_c} = 0 \quad \text{at} \quad z_I = q_c = \tfrac{1}{2} \tag{25}$$

We assert without proof that these conditions indeed represent a minimum. This can be accepted on the basis of physical reasoning or from the numerical results which are given later. Differentiating Equation (23) with respect to z_I, we get

$$\left.\frac{\partial \overline{T}_z}{\partial z_I}\right|_{\frac{1}{2}} = \sum_{m=0}^{\infty} \sum_{n=0}^{\infty} \left[\frac{\lambda_m^2 - \lambda_n^2}{Pg}\right] \mathrm{Exp}\left[\frac{-\lambda_m^2 - \lambda_n^2}{2Pg}\right] \frac{F(\lambda_m)\, F(\lambda_n)\, I(\lambda_m, \lambda_n)}{N(\lambda_m)\, N(\lambda_n)} \tag{26}$$

Note that the $\lambda_m^2 - \lambda_n^2$ term is antisymmetric in m and n. Thus it will cancel out in the double summation if all other terms are symmetric in m and n, and the other terms are visibly symmetric except possibly for $I(\lambda_m, \lambda_n)$. Thus, the first condition in Equation (25) is true if we can show that $I(\lambda_m, \lambda_n)$ is symmetric when $q_c = \tfrac{1}{2}$.

Returning to Equation (21), the coordinate y can be replaced by the flow rate q using Equation (2). The result is

$$I(\lambda_m, \lambda_n) = \tfrac{1}{2} \int_0^1 Q_m(q_2)\, Q_n(q_1)\, dq_2 \tag{27}$$

where $Y(y) = Q(q)$.

From the transformation in Equation (4), we get

$$I = \tfrac{1}{2} \int_0^{q_c} Q_m(q_2)\, Q_n(q_2 + 1 - q_c) dq_2 + \tfrac{1}{2} \int_{q_c}^1 Q_m(q_2)\, Q_n(q_2 - q_c) dq_2 \tag{28}$$

Substituting $u = q_2 - q_c$ in the second integral and noting that q_2 is just a dummy variable of integration, we get

$$I = \tfrac{1}{2} \int_0^{q_c} Q_m(u)\, Q_n(u + 1 - q_c)\, du + \tfrac{1}{2} \int_0^{1 - q_c} Q_m(u + q_c)\, Q_n(u)\, du \tag{29}$$

and for $q_c = \tfrac{1}{2}$

$$I = \tfrac{1}{2}\int_0^{\frac{1}{2}} [Q_m(u)\, Q_n(u+\tfrac{1}{2}) + Q_m(u+\tfrac{1}{2})\, Q_n(u)]du \quad (30)$$

which is clearly symmetric in m and n.

The second condition in Equation (25) is proved by differentiating Equation (23) with respect to q_c. The result is similar to Equation (26) except that the $\lambda_m^2 - \lambda_n^2$ term is replaced by $\partial I/\partial q_c$. It suffices to show that $\partial I/\partial q_c$ is antisymmetric at $q_c = \frac{1}{2}$. We differentiate Equation (29) to obtain

$$\frac{\partial I}{\partial q_c} = \tfrac{1}{2}Q_m(q_c)\, Q_n(1) - \tfrac{1}{2}\int_0^{q_c} Q_m(u)\, Q_n'(u+1-q_c)\, du + \tfrac{1}{2}Q_m(1)\, Q_n(1-q_c) + \tfrac{1}{2}\int_0^{1-q_c} Q_m'(u+q_c)\, Q_n(u)\, du \quad (31)$$

and

$$\left.\frac{\partial I}{\partial q_c}\right|_{\frac{1}{2}} = \tfrac{1}{2}\int_0^{\frac{1}{2}} [-Q_m(u)\, Q_n'(u+\tfrac{1}{2}) + Q_m'(u+\tfrac{1}{2})\, Q_n(u)]du \quad (32)$$

which is antisymmetric as required.

For the case of complete inversion, only the first condition in Equation (25) applies, since complete inversion has no parameter q_c. It is thus only necessary to show that $I(\lambda_m, \lambda_n)$ is symmetric under the transformation of Equation (6):

$$I(\lambda_m, \lambda_n) = \tfrac{1}{2}\int_0^1 Q_m(y_2)\, Q_n(1-y_1)\, dy_2 \quad (33)$$

Substitution of $y_1 = 1 - y_2$ gives

$$I(\lambda_m, \lambda_n) = \tfrac{1}{2}\int_0^1 Q_m(1-y_1)\, Q_n(y_1)\, dy_1 \quad (34)$$

which establishes the symmetry.

The case of complete mixing at $z = z_I$ is developed in a similar manner. The inlet boundary condition for the second zone is $T_2(z_I, y_2) = \bar{T}_1(z_I)$. Equation (23) becomes

$$\bar{T}_2 = \sum_{m=0}^{\infty}\sum_{n=0}^{\infty} \frac{F^2(\lambda_n)\, F^2(\lambda_m)}{N(\lambda_m)\, N(\lambda_n)} \operatorname{Exp}\left[\frac{-\lambda_m^2(1-z_I) - (\lambda_n^2 z_I)}{Pg}\right] \quad (35)$$

The exponential term is symmetric when $z_I = \frac{1}{2}$, and, like the inversion cases, $\bar{T}_2$ has a minimum at this point. This result is easy to generalize to a multizone heat exchanger with perfect mixing between zones. Equal spacing gives an overall minimum in $\bar{T}$ and an overall maximum in Nu. Using Equation (22), it can be shown that the overall Nusselt number for a K zone, equally spaced heat exchanger is

$$(Nu)_{\text{overall}} = pPg\left[\frac{1-\gamma^K}{1+\gamma^K}\right] \quad (36)$$

where Pg is based on the total length L, and

$$\gamma = \frac{pKPg - Nu\,(KPg)}{pKPg + Nu\,(KPg)} \quad (37)$$

For the special case of a round tube with $K = 2$

$$(Nu)_{\text{overall}} = \frac{Nu(2Pg)}{1 + \left[\dfrac{Nu(2Pg)}{4\,Pg}\right]^2} \quad (38)$$

Asymptotic Behavior

At high values of Pg, heat transfer is controlled by a thermal boundary layer very near the tube wall. The well-known Leveque (1928) solution results from linearizing the parabolic velocity distribution to give

$$Nu = 1.75\, Gz^{1/3} = 2.56\, Pg^{1/3} \quad (39)$$

valid for round tubes and high Pg. Although the constant varies with geometry, the cube root dependence in Equation (39) is also observed for flat ducts (Jakob, 1949; Sellers et al., 1956) and for velocity distributions other than parabolic (Porter, 1971).

At high Pg, the bulk fluid temperature is little affected by the thermal boundary layer which is developing along the tube wall. Any mixing scheme which destroys the boundary layer and replaces it with bulk fluid will yield the same results. Thus, partial flow inversion and perfect mixing show the same asymptotic behavior:

$$(Nu)_{\text{overall}} = \frac{1}{L}\sum_{i=1}^{K} (Nu)_i\, \Delta L_i \quad (40)$$

With equal spacing and with constant R so that all the individual Nu are equal

$$(Nu)_{\text{overall}} = Nu(KPg) \quad (41)$$

Using Equation (39), the performance improvement due to the motionless mixers is

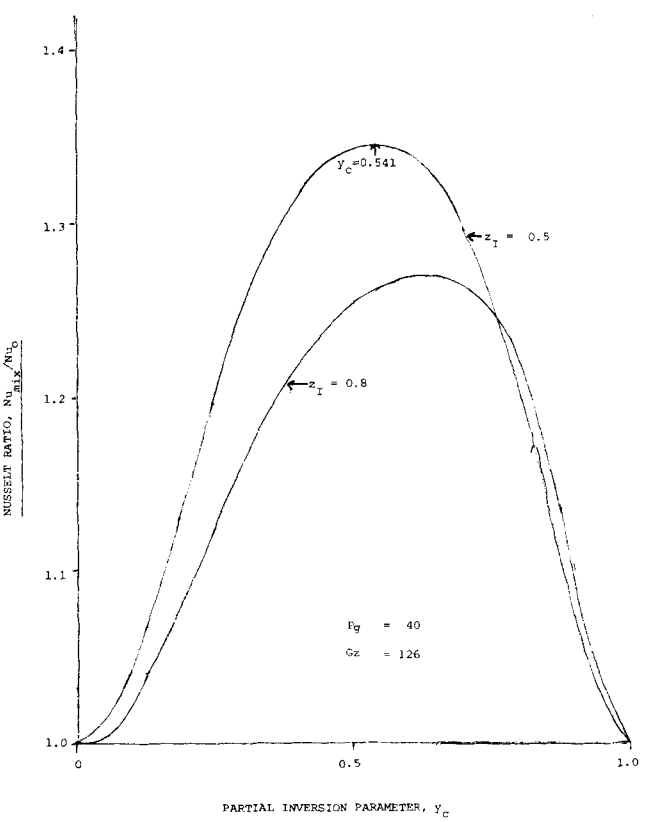

Fig. 6. Optimization of inversion parameter for partial flow inverters.

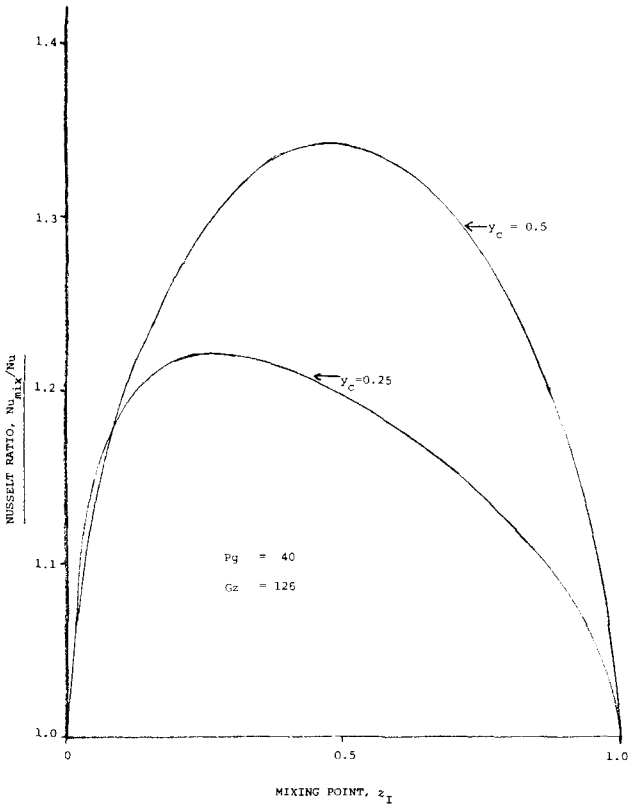

Fig. 7. Optimal mixing point location for partial flow inversion.

$$\frac{(Nu)_{\text{overall}}}{Nu(Pg)} = K^{1/3} \tag{42}$$

This result does not apply to flow dividers until the striation thickness becomes small compared to the thermal boundary layer. It applies to complete inversion only with $K = 2$, since, for higher K, material once near the wall is returned to the wall. Similarly, with partial flow inversion, q_c must be chosen so that fresh material is used to replace the thermal boundary layer. Although not shown to optimal, $q_c = 1 - 1/K$ appears to be a good choice. However, as shown in Appendix A, such flow inverters would be difficult to design for large K. Instead, for very long heat exchangers, it is better to keep the effective K small by interspersing motionless mixers of the conventional type.

NUMERICAL RESULTS

Although the analytical results discussed earlier provide a theoretical solution to the Graetz problem with intermediate mixing, the various sums in Equations (19) through (21) turn out to be quite difficult to evaluate numerically. Practical solutions to this class of problems are better achieved by strictly numerical methods. Finite-difference techniques were used in the present study, and only the round tube geometry was considered.

For the general case of variable physical properties, Equation (9) must be solved simultaneously with the equations of motion. If we assume that $\partial V/\partial z$ is small compared to $\partial V/\partial y$, the equations of motion reduce to the simple form

$$\frac{V(y)}{V_o} = 1 - \frac{\int_0^y \frac{y'}{\mu(y')}\,dy'}{\int_0^1 \frac{y'}{\mu(y')}\,dy'} \tag{43}$$

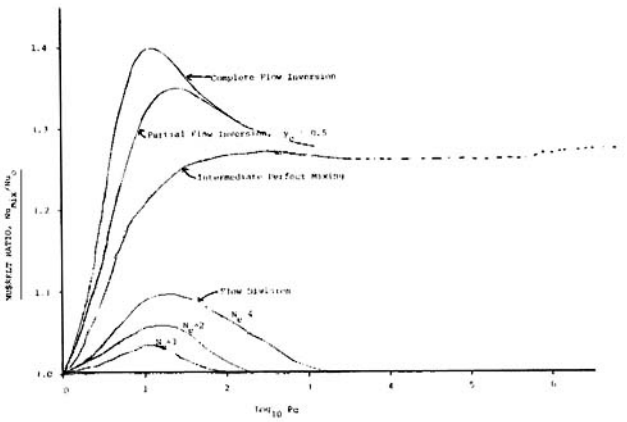

Fig. 8. Nusselt number enhancement with intermediate mixing.

where μ is a function of temperature and thus of radial position y.

For the set of Equations (9) and (43), the easiest approach is to use central differences and a grid which is equally spaced in the y direction. For undisturbed parabolic flow, the numerical results converge quickly and accurately to those for the classical Graetz problem (Sellers et al., 1956; Brown, 1960). With flow inversion or division at $z = z_I$, convergence is delayed owing to difficulties in obtaining a smooth numerical approximation to the transformation $y_1 \rightarrow y_2$ while still maintaining the heat balance requirement that

$$\overline{T}_1(z_I) = \overline{T}_2(z_I) \tag{44}$$

The difficulty arises from the fact that temperatures at the various radial mesh points upstream of the motionless mixer cannot be directly translated to the mesh points downstream of the mixer. Instead, numerical interpolation is needed, and some adjustment to straightforward interpolation is required to ensure that Equation (44) is satisfied. However, computation is still quite feasible with modern computers, and the major practical difficulty is in writing the program logic which performs the coordinate transformation together with the various interpolations and normalizations. Also, iteration is needed at the reactor outlet, since both $V(r)$ and $T(r)$ are unknown [although $T(q)$ is known].

With constant physical properties, $V(r)$ is unchanged by the mixer, and there are substantial theoretical advantages to using a coordinate system which is equally spaced in q and thus unequally spaced in y. With unequally spaced coordinates, the finite-difference form of Equation (9) becomes

$$T_i(z+\Delta z) = T_i(z)\left[1 - \frac{\Delta z}{Pg\,V(y)}\left(\frac{2}{(\Delta y^+)(\Delta y^-)}\right)\right] + T_{i+1}(z)\left[\frac{1}{y_i \Delta y} + \frac{2}{\Delta y\,\Delta y^+}\right] + T_{i-1}(z)\left[\frac{1}{y_i \Delta y} + \frac{2}{\Delta y\,\Delta y^-}\right] \tag{45}$$

where

$$\begin{aligned} \Delta y_+ &= y_{i+1} - y_i \\ \Delta y_- &= y_i - y_{i-1} \\ \Delta y &= \Delta y_+ + \Delta y_- \end{aligned} \tag{46}$$

The logic for the various coordinate transformations $y_1 \rightarrow y_2$ is very simple with equal q spacing, since the flow elements can be interchanged directly. Also, Equation (44) is satisfied automatically. Thus, programming logic

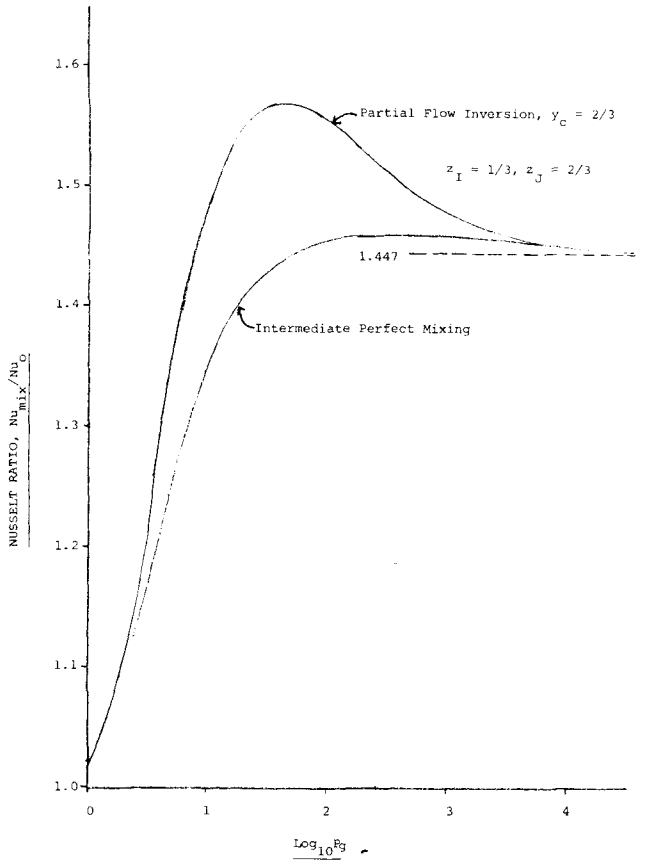

Fig. 9. Three-zone heat exchanger with equally space intermediate mixing.

is much easier with the equal q approach. Unfortunately, convergence turns out to be slower.

PARABOLIC VELOCITY DISTRIBUTIONS

Figure 6 through 8 show calculated results for parabolic velocity distributions in two-zone heat exchangers with various forms of intermediate mixing. The reference condition is undisturbed flow in a heat exchanger of the same total length, that is, with the same value for Pg. Undisturbed flow gives a temperature distribution which is monotone in y. Any form of intermediate mixing destroys this monotonicity and gives higher rates of heat transfer. The degree of enhancement depends on the specific mixing transformation $y_1 \rightarrow y_2$.

Figures 6 and 7 explore the parametric sensitivity of two-zone heat exchangers with partial flow inversion. In Figure 6, y_c is varied at fixed values of z_I. For $z_I = 0.5$, the theoretical optimum occurs at $q_c = 0.5$, $y_c = 0.541$, and this is borne out by the numerical results. For $z_I = 0.8$, the optimal values for q_c and y_c are shifted, but using $q_c = 0.5$ would still be a reasonably good strategy. Figure 7 indicates sensitivity to variations in z_I at fixed values of y_c. For $y_c = 0.5$, the optimum is very near $z_I = 0.5$, but close examination of the underlying data shows a skew toward lower values of z_I as might be expected for the suboptimal y_c. This skewness is much more pronounced for $y_c = 0.25$, where the local optimum is at $z_I = 0.3$. However, even at $y_c = 0.25$, a strategy of having $z_I = 0.5$ would not be particularly bad.

Figure 8 shows the overall enhancement in Nusselt number for a variety of mixing strategies. The uppermost curve is for complete flow inversion at $z_I = 0.5$. It is suspected but not proved that this represents the best possible transformation, $y_1 \rightarrow y_2$. The two-channel, partial flow inverter with $z_I = y_c = 0.5$ is seen to provide a reasonably close approximation to complete inversion. Note that the results in Figure 8 are for $y_c = 0.5$, not $y_c = 0.541$. Achievement of the exact optimum of $q_c = 0.5$ would be difficult owing to uncertainties in the velocity profile and in the design of the inverter. The results in Figure 8 should be quite accurate for q_c in the range 0.45 to 0.55 and are a reasonable approximation for $0.4 < q_c < 0.6$.

The curve for perfect mixing at $z_I = 0.5$ shows this to be a worse strategy than flow inversion at intermediate values of Pg. The better performance with flow inversion is due to the higher driving forces which result from bringing center line material to the walls. The driving force advantage vanishes at either limit of high or low Pg, and thus perfect mixing has the same asymptotic behavior as flow inversion. The situation is quite different for flow division since fluid is undisturbed for a distance of one striation thickness from the wall. At high Pg, the thermal boundary layer is smaller than the striation thickness, so that there is no effect of mixing. Thus, for finite N_e, each flow division curve in Figure 6 shows an asymptote of $Nu_{mix}/Nu_o = 1.0$ for both high and low Pg. The performance of flow dividers can be increased by increasing N_e (the perfect mixing curve in Figure 6 is an upper bound), but at high N_e and high Pg, the length required for the mixer can no longer be considered short compared to that for the heat exchanger. The Nusselt enhancement for a distributed motionless mixer would be lower than for a lumped mixer if the distributed mixer delayed achievement of the final striation thickness beyond $z_I = 0.5$.

Figure 9 shows numerical results for three-zone heat exchangers with intermediate mixing at two points $0 < z_I < z_J < 1$. Complete flow inversion is not a good strategy for a three-zone heat exchanger and is not included in Figure 9. Partial flow inversion with equal spacing, $z_I = 1/3$, $z_J = 2/3$, and with $q_c = 2/3$ is seen to be a reasonably good strategy, substantially outperforming intermediate perfect mixing. Although not shown to be optimal, partial flow inversion with equal spacing and $q_c = 1 - 1/K$ appears to be a good strategy for multizone heat exchangers in general. Also not proved but suspected is that intermediate perfect mixing provides a lower bound on the performance of such a multizone heat exchanger. Thus, Equation (38) should provide a conservative estimate for the Nusselt number.

Temperature Dependent Viscosity

Laminar flow heat exchangers with variable viscosities are much more difficult to characterize than those with a constant viscosity. The temperature dependence of viscosity introduces at least one additional parameter, and the coupling of the temperature profile with the velocity distribution causes the numerical methods to converge more slowly. This paper does not attempt a comprehensive study of the variable viscosity problem but does present selected results which illustrate the general phenomena and which hopefully suggest some guidelines for design.

A temperature dependence of the Arrhenius type was assumed, with the activation energy chosen to yield a desired value for the viscosity ratio μ_0/μ_{wall}. This ratio, although with μ_0 based on average properties rather than inlet properties, is used for the well-known Sieder-Tate (1936) correction to Leveque's equation. The Sieder-Tate correlation found Nu to vary as the 0.14 power of the viscosity ratio, and this remains a good first approximation, although Popovska and Wilkinson (1977) have shown that

TABLE 1. CALCULATED NUSSELT NUMBERS FOR $Pg = 50$

	Viscosity ratio, μ_0/μ_{wall}		
	0.1	1.0	10.0
Undisturbed flow	6.3	8.9	11.2
Partial inversion, $z_I = y_c = .5$	8.8	11.9	13.7
Nusselt ratio	1.39	1.33	1.23
Perfect mixing, $z_I = .5$	7.5	11.2	14.6
Nusselt ratio	1.20	1.26	1.30
Equation (38) prediction	7.4	11.2	14.8

numerical calculations of the type used here provide closer agreement with experimental data.

Table 1 gives calculated Nusselt numbers for $\mu_0/\mu_{wall} = 0.1$ (cooling), 1.0 (parabolic), and 10.0 (heating) for a variety of heat exchanger configurations at $Pg = 50$. Although not optimized, partial inversion with $z_I = y_c = 0.5$ is seen to be a reasonably good strategy for all situations. It shows the greatest benefit when the fluid is being cooled so that the velocity profile is elongated. As in all cases, the flow inverter moves material from the center line to the wall and thus increases the driving force for heat transfer. With cooling, however, flow inversion gives the additional advantage of flattening the velocity profile. This is illustrated in Figure 10 which shows the velocity profiles immediately before and after the inverter and at the exit of the heat exchanger. The inverter is seen to give a distorted but flatter and more favorable velocity distribution at $z = 0.5$ than the parabolic distribution which existed at the heat exchanger entrance $z = 0$. At the exit, the velocity profile has returned to the elongated form, but the elongation is less pronounced than at the inlet to the inverter.

While a partial flow inverter gives a greater advantage for cooling than it does for the constant parabolic distribution, it gives less advantage for heating. Indeed, perfect mixing at $z = 0.5$ is a better strategy than flow inversion. The reason for this is that, for heating, the flow inverter alters the velocity distribution to one less favorable to heat transfer and this overcomes the slightly higher driving force which flow inversion gives compared to perfect mixing.

The perfect mixing results in Table 1 were calculated directly from Equations (9) and (43). It is interesting to compare these Nusselt numbers with those predicted from Equation (38) using Nu calculated for undisturbed flow at half the tube length. The condition for Equation (38) to hold is that the mixing causes the Nusselt numbers to be exactly equal in the two halves of the heat exchanger. This is true for $\mu_0/\mu_{wall} = 1$, since $V(r)$ is identical and constant for both halves. With cooling, $V(r)$ elongates in both halves, but it elongates less in the second half since the bulk fluid has cooled and there is less of a viscosity difference between the centerline and the wall. With cooling, the second half of the heat exchanger has a higher Nusselt number than the first half, and Equation (38) slightly underpredicts $(Nu)_{overall}$. The situation is reversed for heating, and Equation (38) overestimates the overall Nusselt number.

Reviewing the various results presented so far, one concludes that partial flow inversion is an excellent, near optimal strategy for cooling or other situations such as polymerization which give elongated velocity profiles. Partial inversion gives heat transfer coefficients which are at least equal to and usually better than intermediate perfect mixing. For flattened velocity profiles, perfect mixing can give somewhat better results although, in practice, partial

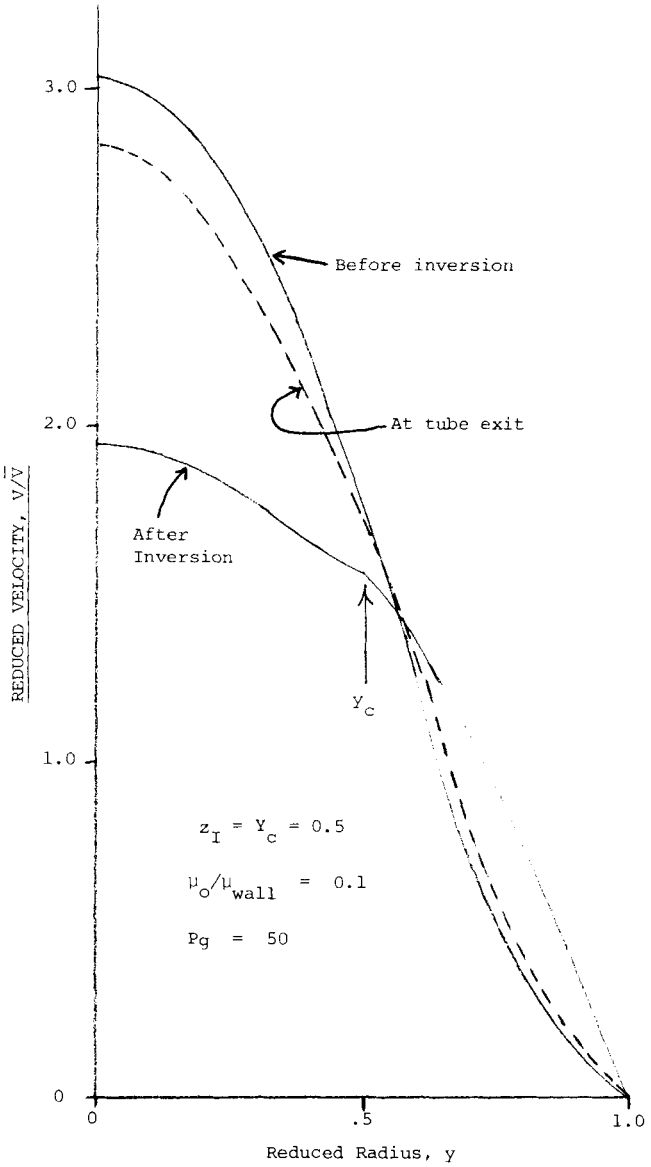

Fig. 10. Velocity profile for partial inversion with cooling.

inverters might still be expected to outperform motionless mixers which are primarily flow dividers.

From a design viewpoint, it is assumed that the basic correlation of Nusselt number with Gratez number or with Pg is known, for example, from the Sider-Tate equation, and the problem is to estimate how much improvement can be expected from a flow inverter. Figures 8 and 9 can be used directly if the velocity profile remains approximately parabolic and should provide conservative estimates if the velocity profile elongates. Alternatively, Equation (36) should provide a conservative estimate of $(Nu)_{overall}$ except for the heating of very temperature sensitive materials. With heating, there is no conservative estimation techniques other than assuming zero enhancement. Accurate design thus requires numerical calculations for the specific situation of interest.

Thermal Time Distributions

When laminar flow heat exchangers are used as reactors, the Nusselt number is not a useful measure of performance. Instead, the reaction environment can be characterized by the thermal time distribution (Nauman, 1977) which is the nonisothermal analogue of the residence time distribution. The thermal time is found by integrating the Arrhenius temperature dependence along a fluid streamline

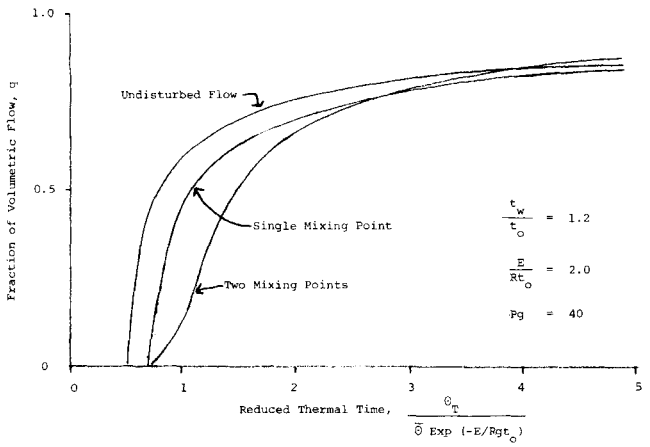

Fig. 11. Effect of partial flow inversion on thermal time distribution.

$$\Theta_T = \int_0^{\Theta} \mathrm{Exp}\,[-E/R_g t(\Theta')]\,d\Theta' \qquad (47)$$

When Θ is found as a function of the volumetric flow variable q, the result can be expressed as a cumulative distribution function analogous to the residence time distribution function. Indeed, for $E/R_g t_o = 0$, these two distributions are identical.

The thermal time distribution can be used to predict yields for nonisothermal reactions in a manner exactly analogous to the way the residence time distribution is used to predict yields in isothermal systems. Thus it is a powerful tool in reactor analysis and tells a great deal about the internal environment from a reaction viewpoint. When the heat of reaction is small, this environment is entirely governed by external heat transfer, and the thermal time distribution can be calculated independently of the details of the reaction. The underlying theory which supports these statements is given elsewhere (Nauman, 1977). For present purposes, the thermal time distribution can be considered a modified residence time distribution which depends on the heat transfer characteristics of the system.

It has been observed that fixed wall heat exchangers give very nonuniform reaction environments. Fluid near the centerline has a low residence time and remains cool so that the thermal time is very short. Material near the wall has long residence times coupled with high temperatures so that Θ_T is very long. The resulting thermal time distribution is extremely broad and gives low reaction yields. Figure 11 shows how partial flow inversion affects this situation. The results, although far from spectacular, indicate some improvement in the uniformity of the reaction environment. The data in Figure 11 are expressed in terms of a reduced thermal time

$$\frac{\Theta_T}{\bar{\Theta}\,\mathrm{Exp}\,(-E/R_g t_o)} \qquad (48)$$

For parabolic flow at high Pg, center line material remains at temperature t_o and has a velocity twice the mean. Thus the reduced thermal time for this material is 0.5. Note that the scaling factor for the data in Figure 11 is not the mean thermal time which varies between the various cases and is about 2.5 in the units used for Figure 11.

A two-zone heat exchanger with intermediate perfect mixing was also evaluated with respect to thermal time distributions. Since the fluid is completely homogenized at the mixing point, the exit thermal time is the sum of two independently distributed random variables: the thermal time experienced in the first half of the heat exchanger and the thermal time experienced in the second half. These two component distributions are very similar but not identical since the second zone of the heat exchanger has a higher average temperature and thus a high average thermal time. Results of the summation give an exit distribution which is very similar to that for a two-zone heat exchanger with partial flow inversion and are not shown separately in Figure 11.

ACKNOWLEDGMENT

Special thanks are due my former employer, Union Carbide Corporation, for releasing the design of the flow inverter shown in Figure 4.

NOTATION

C = constant of integration
D = tube diameter or width of duct
E = activation energy
F = function of eigenvalues defined by Equation (24)
g = geometric parameter; $q = 0$ for ducts, $q = 1$ for tubes
Gz = Graetz number, defined by Equation (11)
h_{ia} = arithmetic mean heat transfer coefficient
k = thermal conductivity
K = number of zones in heat exchanger
L = length of heat exchanger
m, n = indexes of summation
N = normalization parameter, defined by Equation (17)
N_e = number of flow division elements in series
Nu = Nusselt number, $h_{ia} D/k$
$(Nu)_{\mathrm{mix}}$ = Nusselt number for heat exchanger with lumped motionless mixers
p = geometric parameter; $p = 4$ for ducts, $p = 2$ for tubes
Pg = Graetz parameter, defined by Equation (11)
q = reduced volumetric flow rate
q_c = recombination value for partial flow inverter
Q = eigenfunction expressed as a function of q
r = radial coordinate
R = radius of tube or half width of duct
R_g = gas law constant
S = striation thickness
t = absolute temperature
$t(\Theta')$ = absolute temperature measured as function of position and of age Θ'
T = reduced temperature defined by Equation (8)
$\bar{T}$ = mixing cup average value of T
u = dummy variable of integration
v_x = axial velocity component
V = reduced velocity, $v_x/\bar{V}$
V_o = center line velocity
$\bar{V}$ = average value of v_x
W = weighting function; $W = 1$ for flat ducts, $W = 2y$ for round tubes
x = axial coordinate
y = reduced radial coordinate, r/R
y_c = recombination point for partial flow inverter
Y = eigenfunction, defined by Equations (12) and (13)
z = reduced axial coordinate, x/L
Z = separation function, defined by Equations (12) and (13)

Greek Letters

α = thermal diffusivity
β = eigenvalue, $\beta^2 = (V_0/\bar{V})\,\lambda^2$
γ = defined by Equation (37)
Δ = dimensionless thickness of annular spacer

θ = tangential coordinate
Θ = residence time or exit age
$\bar{\Theta}$ = mean residence time
Θ_T = thermal time
λ = separation constant or eigenvalue, defined by Equation (13)
μ = viscosity
ϕ = defined by Equation (A8)
Φ = Graetz parameter used by Jakob, $\Phi = 4Pg$
ψ = dimensionless inside radius of annulus

Subscripts

0 = inlet conditions or undisturbed flow
1, 2 = locations upstream and downstream of a lumped motionless mixer
c = recombination point for partial flow inverter
d = division point for partial flow inverter
i = index of summation
I = location of (first) mixing point
J = location of second mixing point
m = index of summation used for second zone of heat exchanger
n = index of summation used for first zone of heat exchanger
w = wall conditions

APPENDIX A: HYDRODYNAMIC DESIGN CONSIDERATIONS

A rudimentary analysis of the hydrodynamics in a two-channel, partial flow inverter is made possible by dividing the inverter into three regions. Fully developed flow is assumed within each region, and all entrance and transitional effects are ignored. Only Newtonian fluids with constant properties are considered.

The first, most upstream region is an annulus with inside radius $\psi_d R$. The annulus divides the flow into two streams: an inner stream of fraction q_d and an outer annular stream of fraction $q_c = 1 - q_d$. The second region of the inverter is at the midpoint where the two streams are flowing side by side within a circular cross section (see section C-C in Figure 4). The third region of the inverter is again an annulus, but the fraction q_d is now flowing in the outer annular stream while the fraction q_c flows inside. The inside radius in the third region is ψ_c, and, in general, $\psi_c \neq \psi_d$. Note also that the parameters used earlier, y_d and y_c, are not identical to ψ_d and ψ_c. For the undisturbed velocity profile, y_d is the radial position at which the stream is divided into fractions q_d and q_c. In practice, the inverter disturbs the flow so that ψ_d is a physical design parameter used to achieve the desired split. The fact that y_d and ψ_d are different presents a design problem which has only been partially resolved at the present time.

Consider the problem of achieving some q_d which is substantially different from 0.5. This is done by choosing geometrical dimensions such that the two channels will have equal pressure drops when the flow is divided into fractions q_d and q_c. If $q_d \neq q_c$, the inverter must be asymmetric with $\psi_d \neq \psi_c$. Suppose the length of the two annular regions is long so that the total pressure drop through the inverter is dominated by these two regions. Then, the division of the total flow into the fractions q_d and q_c can be based on the known relationships for Newtonian flow in an annulus and a tube. We first find q_d as a function of ψ_d:

$$q_d = \frac{\text{inside flow}}{\text{total flow}} = \frac{(\psi_d - \Delta)^4}{1 - \psi_d^4 + \dfrac{(1 - \psi_d^2)^2}{\ln \psi_d} + (\psi_d - \Delta)^4} \tag{A1}$$

This equation arises by equating the pressure drops within the tube and the annulus. The term Δ represents the finite thickness of the annular spacer expressed as a fraction of the tube radius. The pressure drop in this first region of the flow inverter is conveniently scaled by the pressure drop in an open tube of the same length and diameter:

$$\frac{\Delta P_d}{\Delta P_o} = \frac{q_d}{(\psi_d - \Delta)^4} \tag{A2}$$

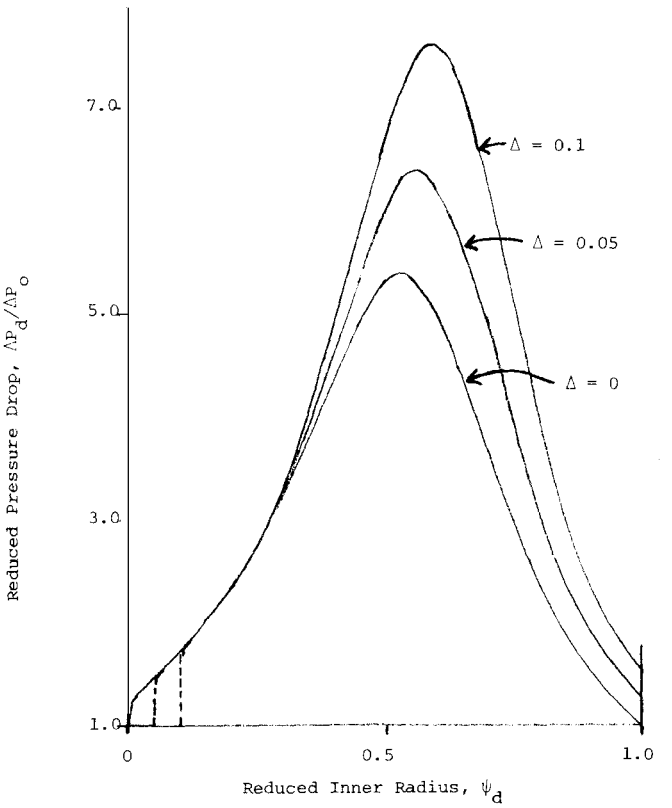

Fig. A1. Pressure drop in annular regions of flow inverter.

The behavior of Equation (A2) is displayed in Figure A1. The maximum pressure drop occurs near but not at the point of equal flow division, $q_d = q_c = 0.5$ A strong function of Δ, this maximum pressure drop is seen to be five to eight times that in an open tube.

In the central region of the inverter, the tube is divided by a chord which is a diameter when there is equal division. Laminar flow in a circular segment is an interesting two-dimensional flow problem which apparently has not been treated in the literature. Thus, it is uncertain how to position the chord to achieve equal pressure drops for the two channels. Although generally unsuited for laminar flow situations, use of the hydraulic mean radius is the only available design approximation. The results should not be too bad if the length of the central region is small compared to that for the annular regions. Pressure drops of four to eight times that in an open tube are expected with equal division.

Flow in the third region of the inverter is identical to that in the first region except that q_d is replaced by q_c. The curves in Figure A1 are roughly symmetrical in terms of q_d and q_c so that the pressure drops in the two annular regions are similar in magnitude. The inverter shown in Figure 4 has a total L/D of 4. Thus, an overall pressure drop equivalent to 20 to 30 tube diameters can be expected.

Table A1 gives solutions of Equation (A1) for $\Delta = 0$ together with the values of y_d which correspond to an undisturbed, parabolic velocity distribution. For equal division, y_d and ψ_d are nearly equal so that only a small amount of radial flow occurs at the entrance on the inverter. For the other q_d, a substantial amount of radial flow is necessary in going from the open tube to the annulus. Also, q_d is seen to be quite sensitive to ψ_d, so that careful mechanical design is necessary to achieve an accurate split in an asymmetric flow inverter. Equation (A1) is approximately linear for ψ_d in the range from 0.4 to 0.65. In this range, q_d varies from 0.1 to 0.8, so that

TABLE A1. DESIGN PARAMETERS FOR PARTIAL FLOW INVERTERS

q_d	y_d	ψ_d	$\Delta P_d/\Delta P_o$	q_c	y_c	ψ_c	$\Delta P_c/\Delta P_o$
0.5000	0.5412	0.5526	5.36	0.5000	0.5412	0.5526	5.36
0.3333	0.4284	0.5006	5.31	0.6667	0.6501	0.6042	5.00
0.2500	0.3660	0.4704	5.10	0.7500	0.7071	0.6337	4.65
0.2000	0.3249	0.4493	4.91	0.8000	0.7435	0.6541	4.37
0.1667	0.2952	0.4332	4.74	0.8333	0.7693	0.6697	4.14

$dq/d\psi$ has a slope of around 3. The effect of $\Delta > 0$ is to offset ψ_d by an amount roughly equal to $\Delta/2$. Thus, $q_d = 0.5$ is achieved with $\psi_d = 0.5526$ when $\Delta = 0$ and with $\psi_d = 0.6062$ when $\Delta = 0.1$.

When the flow inverter is axisymmetric, the pressure drops for the two flow channels will be equal regardless of the value chosen for $\psi_d = \psi_c$. Thus, flow inverters for equal division are relatively easy to make while those for low values of q_d may prove quite difficult, demanding precise hydrodynamic calculations and mechanical accuracy.

APPENDIX B: SOLUTIONS OF THE STURM-LIOUVILLE EQUATION

This section displays solutions to Equation (13) for the four combinations of geometry and velocity profile which have been treated in the literature. The cited eigenfunctions and eigenvalues are those that satisfy the boundary conditions $Y_n(1) = 0$ and $Y_n'(0) = 0$.

Flat Plate Geometry, Flat Velocity Distribution

$$g = 0 \qquad V(y) = 1$$

Sturm-Liouville equation: $Y_n'' + \lambda_n^2 Y_n = 0$

Eigenfunctions: $\cos \gamma_n y$

Eigenvalues: $\lambda_n = (2n + 1)\,\pi/2 = 1.5708, 4.7124, 7.854, 10.9956, \ldots$

Reference: Carslaw and Jaeger (1959)

Flat Plate Geometry, Parabolic Velocity Distribution

$$g = 0 \qquad V(y) = 3/2\,(1 - y^2)$$

Sturm-Liouville equation: $Y_n'' + \beta_n^2\,(1 - y^2)\,Y_n = 0$, $\beta_n^2 = 3/2\,\lambda_n^2$

Eigenfunctions: $$1 - \frac{\beta_n^2}{2}y^2 + \frac{\beta_n^2}{12}\left(\frac{\beta_n^2}{2} + 1\right)y^4 - \frac{\beta_n^4}{360}\left(\frac{\beta_n^2}{2} + 7\right)y^6 + \ldots$$

Eigenvalues: $\beta_n = 1.6816, 5.6699, 9.6682, 13.6677, \ldots$

References: Prins, Mulder, and Schenk (1951). Original solution
Brown (1960). Accurate eigenvalues up to $n = 10$
Sellers, Tribus, and Klein (1956). Asymptotic solution for eigenvalues

Round Tube Geometry, Flat Velocity Distribution

$$g = 1 \qquad V(y) = 1$$

Sturm-Liouville equation: $yY_n'' + Y_n' + \lambda_n^2 y Y_n = 0$

Eigenfunctions: $J_o(\lambda_n y)$ (zero-order Bessel function)

Eigenvalues: $\lambda_n = 2.4048, 5.5201, 8.6537, 11.7915, \ldots$

Reference: Carslaw and Jaeger (1959).

Round Tube Geometry, Parabolic Velocity Distribution

$$g = 1 \qquad V(y) = 2(1 - y^2)$$

Sturm-Liouville equation:

$$yY_n'' + Y_n' + \beta_n^2 y\,(1 - y^2)Y_n = 0,\ \beta_n^2 = 2\lambda_n^2$$

Eigenfunctions: $$1 - \frac{\beta_n^2}{2}y^2 + \frac{\beta_n^2}{16}\left(1 + \frac{\beta_n^2}{4}\right)y_4 - \frac{\beta_n^2}{36}\left[\frac{\beta^2}{4} + \frac{\beta^2}{16}\left(1 + \frac{\beta^2}{4}\right)\right]y_6 + \ldots$$

Eigenvalues: $\beta_n = 2.7044, 6.6790, 10.6734, 14.6711, \ldots$

References: Brown (1960)
Sellers, Tribus, and Klein (1956)

APPENDIX C: ANALYTICAL SOLUTIONS FOR FLOW INVERSION

This section illustrates the evaluation of Equations (19) and (23) for a particular geometry, velocity profile, and coordinate transformation. More specifically, the factors $N(\lambda_n)$, $F(\lambda_n)$, and $I(\lambda_m, \lambda_n)$ are evaluated using the eigenfunctions appropriate to a flat velocity profile between flat plates. Coordinates transformations corresponding to complete inversion and two-channel, partial inversion are treated.

The eigenfunctions are $\cos \lambda_n y$, $\lambda_n = (2n + 1)\pi/2$; the weighting function is $W(y) = 1$; and the velocity profile is $V(y) = 1$. The normalization parameter is obtained from Equation (17):

$$N(\lambda_n) = \int_0^1 \cos^2\left[\frac{(2n+1)}{2}\pi y\right]dy = \tfrac{1}{2} \qquad \text{(C1)}$$

$F(\lambda_n)$ is obtained from Equation (18) with $T(0, y) = 1$:

$$F(\lambda_n) = \int_0^1 \cos\left[\frac{(2n+1)}{2}\pi y\right]dy = \frac{2(-1)^n}{\pi(2n+1)} \qquad \text{(C2)}$$

For complete inversion, the coordinate transformation for the motionless mixer is given by Equation (6) with $q(y)$ being obtained from Equation (2). The result is

$$y_1 = 1 - y_2 \qquad \text{(C3)}$$

Thus, Equation (21) becomes

$$I(m, n) = \int_0^1 \cos\left[\frac{2m+1}{2}\pi y_2\right] \cos\left[\frac{2n+1}{2}\pi\,(1 - y_2)\right]dy \qquad \text{(C4)}$$

$$= \frac{-(2m+1)\,(-1)^m + (2n+1)\,(-1)^n}{2\pi\,(n-m)\,(n+m+1)},\ m \neq n \qquad \text{(C5)}$$

For $m = n$, Equation (C5) is indeterminate, and an alternative form is needed:

$$I(m, n) = \frac{(-1)^m}{\pi(2m+1)},\ m = n \qquad \text{(C6)}$$

Equation (19) can now be written as

$$T_2(z, y_2) = \frac{8}{\pi}\sum_{m=0}^{\infty}\sum_{n=0}^{\infty}$$

$$\frac{(-1)^n I(m,n)\,\mathrm{Cos}\left[\frac{(2m+1)}{2}\pi y^2\right]\mathrm{Exp}\,[\phi]}{2_n+1} \quad \text{(C7)}$$

where $I(m, n)$ is obtained from Equations (C5) or (C6) as appropriate and where

$$\mathrm{Exp}\,\phi = \mathrm{Exp}\left[\frac{-(2m+1)\pi^2(z-z_I)-(2n+1)^2\pi^2 Z_I}{4Pg}\right] \quad \text{(C8)}$$

The $I(m, n)$ term simplifies considerably for specified odd or even values of m and n. This is displayed in the following result for $\overline{T}_2(z)$ which is obtained from Equation (23):

$$\begin{aligned}\overline{T}_2(z) = {} & \frac{16}{\pi^3}\sum_{m=0,2}^{\infty}\sum_{n=0,2}^{\infty}\frac{\mathrm{Exp}\,[\phi]}{(2n+1)(2m+1)(n+m+1)} \\ & + \frac{16}{\pi^3}\sum_{m=0,2}^{\infty}\sum_{n=1,3}^{\infty}\frac{\mathrm{Exp}\,[\phi]}{(2n+1)(2m+1)(n-m)} \\ & - \frac{16}{\pi^3}\sum_{m=1,3}^{\infty}\sum_{n=0,2}^{\infty}\frac{\mathrm{Exp}\,[\phi]}{(2n+1)(2m+1)(n-m)} \\ & + \frac{16}{\pi^3}\sum_{m=1,3}^{\infty}\sum_{n=1,3}^{\infty}\frac{\mathrm{Exp}\,[\phi]}{(2+1)(2+1)(n+m+1)}\end{aligned} \quad \text{(C9)}$$

For the transformation corresponding to two-channel, partial flow inversion, Equation (4) gives

$$\begin{aligned} y_2 &= y_1 - y_c,\ y_2 < q_c \\ y_2 &= y_1 + 1 - y_c,\ y_2 > q_c \end{aligned} \quad \text{(C10)}$$

The following results have been obtained for $I(\lambda_m, \lambda_n)$:

$$I(m,n) = \frac{(-1)^n}{2\pi(n-m)(n+m+1)}$$

$$\begin{aligned}&[(2n+1)\,\mathrm{Cos}\,\lambda_m y_c - (2n+1)\,\mathrm{Cos}\,\lambda_m y_c \\ &\quad - (-1)^m(2m+1)\,\mathrm{Sin}\,\lambda_n y_c \\ &\quad + (-1)^n(2m+1)\,\mathrm{Sin}\,\lambda_m y_c]\end{aligned} \quad \text{(C11)}$$

for $m \neq n$. As before, this is indeterminate for $n = m$, and an alternate result is needed:

$$I(m,n) = (-1)^n\frac{y_c}{2}\,\mathrm{Sin}\,\lambda_n y_c + \frac{(1-y_c)}{2}\,\mathrm{Cos}\,\lambda_n y_c \quad \text{(C12)}$$

for $m = n$.

LITERATURE CITED

Brown, G. M., "Heat or Mass Transfer in a Fluid in Laminar Flow in a Circular or Flat Conduit," *AIChE J.*, **179**, 6 (1960).

Carslaw, H. S., and J. C. Jaeger, *Conduction of Heat in Solids*, 2 ed., Oxford University Press, England (1959).

Jakob, M., *Heat Transfer*, p. 451-464, Wiley, New York (1949).

Leveque, M. A., "Les Lois de la Transmission de Chaleur Par Convection," *Annales Des Mines*, Series 12, 13, 201 (1928).

Nauman, E. B., "Nonisothermal Reactors: Theory and Application of Thermal Time Distributions," *Chem. Eng. Sci.*, **32**, 359 (1977).

Popovska, F., and W. L. Wilkinson, "Laminar Heat Transfer to Newtonian and Non-Newtonian Fluids in Tubes," *ibid.*, 1155 (1977).

Porter, J. E., "Heat Transfer at Low Reynolds Numbers," *Trans. Inst. Chem. Engrs.*, **49**, 1 (1971).

Prins, J. A., J. Mulder, and J. Schenk, "Heat Transfer in Laminary Flow Between Parallel Plates," *Appl. Sci. Res.*, **A2**, 431 (1951).

Sellers, J. R., M. Tribus, and J. S. Klein, "Heat Transfer to Laminar Flow in a Round Tube or Flat Conduit—The Graetz Problem Extended," *Trans. ASME*, **78**, 441 (1956).

Sieder, E. N., and G. E. Tate, "Heat Transfer and Pressure Drop of Liquids in Tubes," *Ind. Eng. Chem.*, **28**, 1429 (1936).

Manuscript received June 2, 1978; revision received October 9, and accepted November 13, 1978.

Properties of Recirculating Turbulent Two Phase Flow in Gas Bubble Columns

The equation of motion for the two phase flow within a bubble column, operated within the recirculation flow regime, has been solved, and the profile of liquid flow has been determined. Nicklin's relation for the bubble flow regime has been extended to the recirculation flow regime.

Data analysis shows that the mean slip velocity between bubble and liquid is approximately constant and that the kinematic turbulent viscosity increases rapidly with increasing diameter of the column. These observations lead to the conclusion that scale-up has but little influence upon the mean gas holdup.

KOREKAZU UEYAMA

and

TERUKATSU MIYAUCHI

Department of Chemical Engineering
University of Tokyo
Tokyo 113, Japan

SCOPE

It is well known that a swarm of bubbles rises uniformly within a gas bubble column when the superficial gas velocity is low (usually less than 2 to 4 cm/s) and when bubbles of uniform size are generated at the gas distributor, that is, when the column is operated in the bubble flow regime. Operation of the column in the bubble flow regime has been utilized widely for several gas-liquid contacting operations (Østergaard, 1968; Sada, 1969; Kumar and Kuloor, 1970).

When the gas velocity is increased, the bubble flow ceases to be uniform; it becomes unstable, intense recirculation is observed within the gas-liquid mixed phase,

Correspondence concerning this paper should be addressed to Terukatsu Miyauchi.